How Fast Is Excitation Energy Transfer in the Photosystem II Reaction Center in the Low Temperature Limit? Hole Burning vs Photon Echo

ARTICLE *in* THE JOURNAL OF PHYSICAL CHEMISTRY B · FEBRUARY 2003

Impact Factor: 3.3 · DOI: 10.1021/jp022231t

6 AUTHORS, INCLUDING:

Valter Zazubovich
Concordia University Montreal
43 PUBLICATIONS **714** CITATIONS
SEE PROFILE

Ryszard Jankowiak
Kansas State University
193 PUBLICATIONS **4,758** CITATIONS
SEE PROFILE

How Fast Is Excitation Energy Transfer in the Photosystem II Reaction Center in the Low Temperature Limit? Hole Burning vs Photon Echo

V. Zazubovich,[†] R. Jankowiak,[†] K. Riley,[†] R. Picorel,[§,‡] M. Seibert,[‡] and G. J. Small*[,†]

Ames Laboratory, U.S. Department of Energy and Department of Chemistry, Iowa State University, Ames, Iowa 50011, National Renewable Energy Laboratory, Golden, Colorado 80401, and E. E. Aula Dei, CSIC, Apdo. 202, 50080 Zaragoza, Spain

Received: October 15, 2002

The $Q_y(S_1)$ excitonic structure, excitation energy transfer (EET), and primary charge-transfer separation processes of the isolated photosystem II reaction center (PS II RC) have proven to be formidable problems due, in part, to the severe spectral congestion of the $S_o \rightarrow Q_y$ absorption spectrum. Recently, Prokhorenko and Holzwarth (*J. Phys. Chem. B* **2000**, *104*, 11563) reported interesting femtosecond 2-pulse photon echo data on the RC at 1.3 K for excitation wavelengths between 676 and 686 nm. At times longer than ∼1 ps and $\lambda \gtrsim 678$ nm, the echo decay curves are highly dispersive, which was attributed to a distribution of primary charge separation rates ranging from 2 ps to several hundred ps. A prompt subpicosecond component of the echo decay curves was also observed and suggested to be due to EET occurring in ∼100−200 fs. We present here persistent nonphotochemical hole burned spectra and transient triplet bottleneck hole spectra obtained with burn wavelengths between 680 and 686 nm, which show that the EET time in that wavelength region is no shorter than ∼5−10 ps. It is argued that the prompt component of the echo decay curves is due to relaxation of low-frequency phonons excited by the pump pulse. The argument is based on hole burning spectroscopy being the frequency domain equivalent of 2-photon echo spectroscopy, as well as on published photon echo data for chromophores in amorphous hosts.

1. Introduction

The $Q_y(S_1)$ excitonic structure, excitation energy transfer (EET), and primary charge separation rates of the isolated D_1/D_2-cyt b_{559} photosystem II (PS II) reaction center (RC) have been the subjects of many frequency and time domain spectroscopic studies since its isolation from spinach in 1987[1] (for a recent review see Dekker and van Grondelle[2] as well as Prokhorenko and Holzwarth[3]). The recent 3.8 Å resolution X-ray structure of Zouni et al.,[4] which is similar to the model structure of Svensson et al.,[5] confirmed that the RC contains six chlorophyll *a* (Chl) and two pheophytin *a* (Pheo) molecules. Two of the Chl molecules, often referred to as Chl_{Z1} and Chl_{Z2}, are peripheral and bound to the D_1 and D_2 polypeptides via histidine residues; analogous bacteriochlorophyll (BChl) molecules are absent in the bacterial RC.[7] A view of the other four Chl and two Pheo molecules (core chlorins) of the PS II RC based on the structure of Svensson et al. is shown in Figure 1. The structural arrangement is similar to that in the bacterial RC. The P_1 and P_2 Chl molecules are analogous to P_L and P_M, the special BChl pair of the bacterial RC, whose lowest excited dimer level (P*) is the primary electron donor state. (The D_1 and D_2 polypeptides are the equivalent of the L and M polypeptides of the bacterial RC; Chl_1, Chl_2, $Pheo_1$, and $Pheo_2$ correspond to $BChl_L$, $BChl_M$, $BPheo_L$, and $BPheo_M$ of the bacterial RC.)

An important difference between the PS II and bacterial RC is that the Mg···Mg distance between P_1 and P_2 is 10 Å, which is 2.4 Å longer than the distance between P_L and P_M. Thus, the excitonic coupling (electrostatic, electron exchange) between P_1 and P_2 is much weaker than the coupling between P_L and P_M. At liquid helium temperatures, the coupling between P_L and P_M of the purple bacterium *Rhodobacter sphaeroides* is ∼700 cm^{-1} (ref 8), while excitonic calculations have led to a value of ∼150 cm^{-1} for P_1 and P_2 (see Jankowiak et al.[9] and references therein). The relatively weak P_1-P_2 coupling and even weaker pairwise couplings involving P_1, P_2, and other chlorins,[9−12] together with the fact that the site excitation energies of the eight chlorins are similar, results in a spectrally congested Q_y absorption spectrum. The inset of Figure 1 shows the 4.2 K absorption spectra of RC-6 and RC-5 which denote, respectively, the PS II RC with the full complement of eight

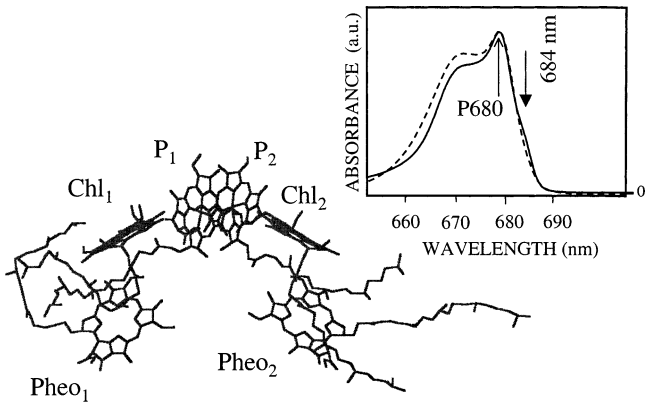

Figure 1. Structural arrangement of the core cofactors in PS II RC based on the structure by Svensson et al.[5] The subscripts 1 and 2 indicate binding to D_1 or D_2 polypeptides. The inset shows the Q_y absorption spectra of RC-5 (solid curve) and RC-6 (dashed curve) at 5 K.

* Corresponding author. E-mail: gsmall@ameslab.gov.
† Ames Laboratory.
‡ National Renewable Energy Laboratory.
§ E. E. Aula Dei.

10.1021/jp022231t CCC: $25.00
Published on Web 02/28/2003

cofactors (six Chl molecules) and the RC with one of the two peripheral Chls that absorbs near 667 nm removed[12] (five Chl molecules). The band labeled by P680 is that of the primary electron donor. In early works it was assumed, by analogy with the bacterial RC, that P680 is due solely to P_1 and P_2. However, recent excitonic calculations on the Q_y structure of the core chlorins (the two peripheral Chls being safely neglected because of their peripheral locations), which take into account diagonal energy disorder due to structural heterogeneity, have revealed that the Q_y states are delocalized over ~3 chlorins (see ref 9 and references therein). The results in ref 9, based on the X-ray structure and the model structure of Svensson et al., predict that, on average, P_1 and P_2 make the largest contributions (~30% each) to P680* (* indicating excited state), but that the contributions from Chl_1 and $Pheo_1$ are significant. The composition of P680* and the other Q_y states were found to vary significantly from complex to complex. Thus, the state of affairs for the PS II RC is much more complicated than for the bacterial RC where absorption bands attributable to the upper and lower dimer levels of P_L and P_M and transitions highly localized on the other cofactors are assignable (see ref 13 and references therein). While the 4.2 K Q_y absorption spectrum of the isolated RC from the purple bacterium *R. sphaeroides* spans a range of ~2700 cm^{-1}, the Q_y spectrum of the PS II RC spans a range of only ~600 cm^{-1} (Figure 1). As discussed in refs 2 and 3, spectral congestion of the Q_y states has made interpretation of time and frequency domain data on the dynamics of primary charge separation and EET in the PS II RC difficult.

Concerning the primary charge separation rate, its value at temperatures near room temperature remains an unsettled issue, with values of ~3 ps^{-1} (refs 14−17), 8 ps^{-1} (ref 18), 0.4 ps^{-1} (ref 19), and 21 ps^{-1} (ref 20) having been reported. At temperatures at or close to 4 K the situation is clearer, with several groups having reported rates in the 2−5 ps^{-1} range.[19,21−26] The triplet bottleneck hole burned (TBHB) spectra in ref 26 led to a value of 4.6 ± 0.4 ps^{-1} for both RC-5 and RC-6 at 5.0 K, establishing that removal of one of the two peripheral Chls does not affect the primary charge separation rate. The 1.3 K two-pulse photon echo decay curves of Prokhorenko and Holzwarth[3] are interesting in that they are dispersive (nonsingle exponential). Theoretical analysis of the dispersive kinetics led to the conclusion that primary charge separation occurs in times ranging from ~2 ps to several hundred ps. The dispersive nature of the decay curves was attributed to structural heterogeneity that results in the composition of P680* (and presumably also the free energy gap associated with the initial phase of charge separation) to vary significantly from RC to RC. Equally interesting is that the echo decay curves exhibit a prompt (subpicosecond) component that Prokhorenko and Holzwarth suggested is due to EET occurring in ~100−200 fs.

In this paper we present TBHB and persistent nonphotochemical hole burned (NPHB) spectra obtained at 5.0 K, which are used to test the assertion that EET in the low-temperature limit occurs as fast as ~100−200 fs. Earlier NPHB studies[21,22,27] led to EET times considerably longer than 1 ps. However, in those works the widths of the zero-phonon holes (ZPH) used to determine the EET rate were obtained with shallow ZPH (≲10% hole depth) so as to eliminate the effect of fluence broadening.[28,29] Because the induced absorption rate of the zero-phonon line (ZPL) is inversely proportional to the homogeneous width of the ZPL (1/2 the width of the ZPH), it can be argued that in the shallow burn limit a broad hole associated with a ~100−200 fs relaxation time was simply not produced. The spectra reported here prove that EET in the 680−686 nm spectral region (Figure 1) occurs no faster than about 10 ps. The spectra were obtained during the course of experiments designed to determine the nature of the Chls responsible for the relatively weak red absorption in the Q_y absorption spectrum at ~684 nm, Figure 1. Several assignments for the 684 nm absorption have been proposed,[2] including that it is due to one of the peripheral Chls,[30] that it is the origin band of the primary donor with the peak in the absorption spectrum at 680 nm seen in Figure 1 associated with one-quantum transitions due to low frequency (~ 80 cm^{-1}) modes[2] and that it is a remnant of the in vivo primary donor origin absorption band located at ~684 nm.[31] Our conclusion regarding this matter will be published elsewhere.[32] Here it is only important to know that the 684 nm band exists in both isolated RC-5 and RC-6 [30,33] and that its assignment is important for understanding the transport dynamics of the isolated PS II RC. It is worth noting that all excitonic calculations involving only the core cofactors predict that the lowest energy Q_y state (P680*) is the most strongly absorbing.

2. Experimental Section

The PS II RC-5 complex was isolated from spinach and purified according to refs 12 and 30. Glycerol (66 vol %) was added to the sample to ensure good glass quality upon cooling to 5.0 K in a Janis 8-DT Super Vari-temp liquid helium optical cryostat. Temperature was controlled and measured using a Lakeshore model 330 controller.

The hole burning setup used is described in ref 30. Briefly, pre-burn and post-burn absorption spectra were recorded with a Bruker HR 120 Fourier transform spectrometer at a resolution of 0.5 cm^{-1}. A CW Coherent CR699-29 dye laser (line width of 0.07 cm^{-1}) pumped by a 6 W Coherent Innova Ar-ion laser was used for hole burning. The burn wavelengths (λ_B) used were 680.0, 682.0, 684.0, and 686.0 nm (see Figure 2), with burn intensities (I_B) ranging between 2 and 700 mW/cm^2, as measured with an NRC model 1825 C power meter. Persistent NPHB spectra at each wavelength were obtained with six burn fluences ranging from ~2.4 to 1800 J/cm^2. At each λ_B value the TBHB spectra were obtained with burn intensities I_B = 2, 40, 200, and 600−700 mW/cm^2.

All reported hole spectra are for one and the same sample. Earlier hole burning studies of the isolated PS II RC with λ_B in the vicinity of 680 nm had shown that both *persistent* NPHB and *transient* TBHB occur,[21,30] with the latter due to formation of the triplet state of the primary donor (^{3}P680*) via charge recombination of the radical ion pair $P680^+Pheo_1^-$. The two types of hole spectra are easily distinguished, in part because the electron−phonon coupling associated with the TBHB spectra is considerably stronger than that of the NPHB spectra (vide infra). To obtain a "pure" TBHB spectrum, it is necessary to first saturate the ZPH of the NPHB spectrum, saturation meaning maximum hole depth.[21] The protocol followed in this work was to first burn six persistent NPHB spectra at a given λ_B with varying burn fluence, starting with the lowest fluence and ending with the highest fluence that was sufficient to saturate the ZPH. Following that the TBHB spectrum (defined here as the absorption spectrum with the laser on minus the absorption spectrum with laser off, sometimes referred to as the triplet−singlet spectrum) was measured with the highest burn intensity used. TBHB spectra were then obtained with the lower burn intensities. As in refs 26 and 30, we confirmed that spontaneous and light-induced filling of the persistent NPHB spectrum during the course of obtaining the TBHB spectra did not contaminate the TBHB spectra. Following the hole burning at a given λ_B value, the sample was warmed to ~150 K to remove hole

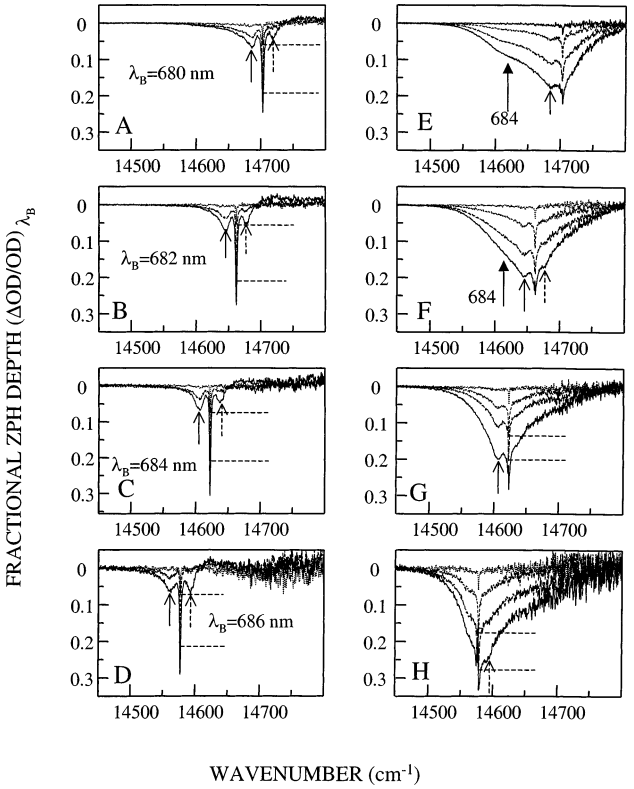

Figure 2. Frames A−D: Persistent hole spectra for $\lambda_B = 680$, 682, 684, and 686 nm, respectively. Burn fluences are 2.4 J/cm^2 for dotted curve, 170 J/cm^2 for dashed curve and 1600−1800 J/cm^2 for solid curve. Frames E−H: Triplet bottleneck hole spectra for $\lambda_B = 680$, 682, 684, and 686 nm, respectively. Burn intensities are 2, 40, 200, and 600−700 mW/cm^2. Vertical solid arrows indicate pseudo-PSBH peaked at 17 cm^{-1} from ZPH. Vertical dashed arrows indicate the real-PSBH. Dashed horizontal lines represent the depths of the ZPH that are obscured by deeper holes (see text). In frames E and F the solid arrows indicate the broad satellite hole due to the 684 nm absorbing Chl.

structure and recooled to 5.0 K. The resulting absorption spectrum was identical to that of the sample before hole burning.

3. Results and Discussion

Figure 2 shows NPHB spectra (A−D) and TBHB spectra (E−H) for $\lambda_B = 680$, 682, 684, and 686 nm; the ordinate is fractional hole depth. The burn fluences (NPHB) and burn intensities (TBHB) used are given in the figure caption. For clarity only three of the six NPHB spectra obtained at each λ_B value are shown. The horizontal dashed lines in frames A−D locate the peak intensity of the ZPH for the upper two spectra, while in frames G and H they locate the ZPH intensity for the middle two spectra. The sharp feature in each frame is the ZPH coincident with λ_B. The solid and dashed arrows locate the pseudo-phonon sideband hole (PSBH) and real-PSBH, respectively, which are displaced by $\sim \pm 17$ cm^{-1} from the ZPH. The real-PSBH builds, in a Franck−Condon sense, on the ZPH.[34,35] The pseudo-PSBH is due to states whose ZPL lies to lower energy of the laser frequency and which absorb via their phonon sideband.[34,35] The spectra in frames A, B, E, and F are similar to those reported earlier [26,30] with λ_B at or in the near vicinity of 680 nm. The TBHB spectra are due to ^{3}P680* formed by charge recombination of P680$^+$Pheo$_1^-$. Theoretical simulations[36] showed that the TBHB spectra are consistent with strong electron−phonon coupling (associated with the $S_o \rightarrow {}^1$P680* transition) with a Huang−Rhys factor (S) of 1.9 for phonons at $\sim$20 cm^{-1}. Thus, the coupling is strong although not as strong as for the primary donor absorption band of *R. sphaeroides* (P870) and *Rhodopseudomonas viridis* (P960), both purple bacteria, and P700 of photosystem I of higher plants, as reviewed in ref 13. Our preliminary simulations of the NPHB spectra in Figure 2 using the theory in ref 34 yielded $S \sim 0.6$ for the 17 cm^{-1} phonon, in good agreement with the values reported in ref 27. Thus, the coupling is quite weak. The first assignment of the NPHB spectra obtained with λ_B at or near 680 nm was to a Q_y-state localized on Pheo$_1$, which can transfer energy to P680 in about 50 ps.[37] However, the excitonic calculations referred to in the Introduction do not predict a state highly localized on Pheo$_1$. Thus, this assignment must be questioned.

The ZPH action spectra (NPHB) presented in ref 30 establish that at 684 and 686 nm the absorption is dominated by the 684 nm absorbing Chl, i.e., the tail of the P680 nm absorption band is essentially negligible at those wavelengths. Based on the action spectrum, which is a direct reflection of the site excitation energy distribution function (SDF) due to structural heterogeneity, the SDF of the 684 nm absorbing Chl is centered at $\sim$684 nm with an inhomogeneous width of $\sim$100 cm^{-1}. The high resolution (<10 MHz) spectra in ref 27 exhibited ZPH widths (shallow burn limit) of $\sim$1 GHz (0.03 cm^{-1}) at 2 K. This width, if attributed to population decay (T_1), leads to a lifetime of 300 ps ($T_1 = (\pi c \Gamma)^{-1}$ where Γ is the width (fwhm) of the ZPH in cm^{-1} and c is the speed of light). However, the temperature dependence (1.3−4.2 K) of the ZPH width established that the width is determined by pure dephasing due to coupling of the electronic transition ($S_0 \rightarrow Q_y(S_1)$) with the two-level systems of the protein.[27] That is, EET does not contribute to the hole width. For this reason Völker and co-workers referred to the 684 nm absorption as being due to a trap state of the isolated PS II RC, incapable of downward EET. TBHB spectra were not reported in their papers.

The results in Figure 2 are very interesting in that they show that the structure of the NPHB spectra and that the structure of the TBHB spectra are similar for all burn wavelengths. Of particular importance is that the spectra for $\lambda_B = 684$ and 686 nm establish that the 684 nm absorption band consists of two subsets of Chl molecules, one giving rise to TBHB spectra of the type associated with primary charge separation (strong electron−phonon coupling, vide supra), and another responsible for persistent NPHB. Thus, the situation for the above two wavelengths is similar to that for $\lambda_B = 680$ nm, near the maximum of the P680 absorption band. (We note that the $\lambda_B = 680$ and 682 nm TBHB spectra (frames E,F) exhibit a broad, nonline narrowed hole due to the 684 nm Chl as reported in ref 30. This hole could result from excitation of low-frequency vibrational modes associated with the 684 nm Chl followed by rapid relaxation to the zero-point level and/or from EET from states excited at λ_B to the 684 nm Chl; as expected the broad 684 nm hole vanishes for $\lambda_B = 684$ nm and longer wavelengths.) The implications of the spectra in Figure 2 for the nature of the 684 nm Chl will be considered elsewhere.[32] Here we focus on the widths of the ZPH in the spectra. Again, the motivation was to test the proposal of Prokhorenko and Holzwarth that EET processes triggered by excitation in the 680−686 nm region occur in $\sim$200 fs in the low-temperature limit. For what follows we note that an EET time of 200 fs corresponds to a ZPH width of 50 cm^{-1}.

The ZPH of the lowest spectrum in each of the frames in Figure 2 are saturated. The fractional depths of the saturated ZPH in frames A−D (NPHB) are 0.25, 0.28, 0.31, 0.29, respectively. In frames E−H (TBHB) they are 0.21, 0.25, 0.28, and 0.32, respectively. Thus, NPHB and TBHB in combination

results in a fractional hole depth of ~0.5−0.6 at λ_B. Based on the Huang−Rhys factors (S) for low frequency phonons given earlier, it follows that essentially all of the ZPLs have been burned, with the remaining absorption at λ_B due to phonons. The widths (fwhm) of the saturated NPHB holes in frames A−D are 3.1, 2.6, 2.1, and 2.1 cm^{-1}, respectively. They are ~25× narrower than expected for EET occurring in 200 fs. Because the holes are saturated they suffer from fluence broadening. With such broadening, together with a read resolution of 0.5 cm^{-1}, we estimate that a hole width of ~1 cm^{-1} is a reasonable value for determining a lower limit for EET times in the 680−686 nm region, which is 10 ps. The widths of the ZPH in the TBHB spectra for the lowest spectrum in frames E−H (obtained with a burn intensity of 700 mW/cm^2) could not be determined reliably because of a noise spike at λ_B due to a small amount of laser light reaching the detector of the FT spectrometer. Nevertheless, the widths are certainly no broader than 5 cm^{-1}. The widths for the second lowest spectrum in frames E−H obtained with a burn intensity of 200 mW/cm^2 are 3.9, 3.8, ~2.4, and 2.7 cm^{-1}, respectively. We emphasize that in all previous TBHB studies with λ_B at or near 680 nm, the width of the ZPH has been attributed to the initial phase of primary charge separation. (This is also the case for the RC of the purple bacteria *R. sphaeroides* and *R. viridis*; for a review see ref 13 in which it is emphasized that the rate of the initial phase of charge separation in the low-temperature limit determined by TBHB is in excellent agreement with the rate determined by fs pump−probe spectroscopy.) The above widths are undoubtedly contributed to by fluence broadening as discussed in ref 26 for TBHB spectra obtained with $\lambda_B = 680$ nm. In that work a procedure for obtaining the homogeneous width of the ZPH is given. Taking 2 cm^{-1} as a reasonable estimate of this width in the 680−686 nm regime and assuming that it is due to EET rather than charge separation leads to a lower limit of 5 ps for the EET time.

4. Discussion and Concluding Remarks

The hole spectra presented prove that in the isolated PS II RC EET involving Q_y states excited at wavelengths between 680 and 686 nm occurs no faster than ~5−10 ps in the low-temperature limit. This finding is in disagreement with the suggestion of Prokhorenko and Holzwarth[3] that EET occurs about twenty times faster. The striking disagreement between the results of the photon echo and hole burning experiments begs an explanation. As mentioned, the high quality echo decay curves in ref 3 are dispersive and exhibit a prompt subpicosecond decay that Prokhorenko and Holzwarth attribute to EET. The highly dispersive part of the decay that occurs at times longer than ~1 ps was attributed to primary charge separation for excitation wavelengths ≳678 nm. A key finding of Prokhorenko and Holzwarth is that the prompt component of the decay is observed even at 686 nm, at the red edge of the absorption spectrum (Figure 1). They briefly note that this is inconsistent with EET since at the red edge EET processes should be absent, but do not consider the consequences of this. The possibility that the prompt component is due to relaxation of excited phonons that relax on a subpicosecond time scale was not considered. In the absence of slow spectral diffusion processes, the 2-pulse echo experiment is the time domain equivalent of the hole burning experiment.[38,39] Thus, the phonon structure seen in Figure 2 should be reflected in the echo decay curves.[39] It is well established that in the low-temperature limit the echo decay curves of chromophores in solids exhibit a prompt decay due to the phonon sideband that accompanies the zero-phonon line (ZPL) followed by a slower decay due to electronic dephasing. The reader is referred to the recent paper by Vainer et al.[40] in which 2-photon and incoherent echo decay curves are presented for Zn-octaethyl porphine in glassy toluene (1.7−100 K). The prompt decay due to low-frequency phonons occurs in ~100 fs with a relative amplitude governed by $1 - \exp(-S(T))$ which is the T-dependent Franck−Condon factor for the phonon sideband. This factor for the ZPL is $\exp(-S(T))$. In accordance with theory,[39] the results of Vanier et al. show that as T increases the amplitude of the decay due to phonons increases while the amplitude due to the ZPL decreases. The best example of the equivalent of this in hole burning is for Al-phthalocyanine tetrasulfonate in hyperquenched glassy water.[41] The theoretical analysis of Prokhorenko and Holzwarth used a value for $S(T = 0\ K)$ of 1.8, which means that even in the low-temperature limit the absorption throughout the entire Q_y absorption is dominated by phonon rather than ZPL transitions. It should be noted that as the excitation frequency in the echo experiment is tuned to higher energy within the Q_y absorption spectrum one expects to see a shortening of the decay of the prompt component due to phonons, which is consistent with the results of Prokhorenko and Holzwarth. The relaxation time of the phonon sideband can be estimated using the width of the real-PSBH in hole spectra. The NPHB spectra in Figure 2 give directly a width of ~15 cm^{-1} for the 17 cm^{-1} phonon. Theoretical simulations of TBHB spectra had yielded a value of ~30 cm^{-1} for the active ~20 cm^{-1} phonon.[36] Both are the widths of the one-phonon profile. The average of the two widths corresponds to a relaxation time of ~200 fs. We note that the fluorescence line-narrowed spectra of Peterman et al.[42] revealed also a phonon sideband at 80 cm^{-1} with a width of ~100 cm^{-1} which corresponds to a relaxation time of ~50 fs.

In view of the hole burned spectra and above discussion of the importance of phonon relaxation to the initial decay of the echo amplitude, we conclude that the upper limit for EET rates in the isolated PS II RC is ~5−10 ps^{-1} in the low-temperature limit for excitation between 680 and 686 nm and that the prompt component of the echo decay curves of Prokhorenko and Holzwarth[3] is due primarily to phonon relaxation processes. It appears, therefore, that the highly dispersive kinetics of the echo decay curves observed for times longer than ~1 ps is most likely also contributed to by a distribution of EET rates (in addition to a distribution of primary charge separation rates). We emphasize that the photon echo data in ref 3 are important for understanding the excitonic structure and transport dynamics of the PS II RC as will be discussed elsewhere.[32] In that paper the burn fluence and burn intensity dependencies of the NPHB and TBHB spectra in Figure 2 will also be discussed.

Finally, we emphasize that the hole spectra presented here do not speak to EET rates for excitation at wavelengths shorter than 680 nm within the Q_y absorption spectrum. The possibility that EET times for such wavelengths are much shorter than ~5−10 ps in the low-temperature limit cannot be excluded. Based on transient absorption spectra at room temperature, it was concluded that energy equilibration occurs in ~100 fs at 670 nm (also 680 nm),[20,43,44] but at this time it is not possible to accurately predict the temperature dependence of the equilibration processes. Völker and co-workers, on the basis of NPHB data (1.2 K), identified ~10 ps downward EET with excitation between 665 and 673 nm. Relatively low burn fluences were used. It is possible that a much shorter EET time[27] distribution could be identified with high burn fluences, although it would probably be difficult to identify the corresponding broad ZPH due to interference from the broad phonon sideband hole

structure associated with the ZPH whose width is determined by 10 ps EET. A related problem for the 2-pulse photon echo is distinguishing between subpicosecond decay due to EET and decay due to phonons. We note that picosecond transient absorption studies (15 K − room temperature) identified 10−20 ps EET times in the 665−673 nm wavelength region.[16,24,44,45,46] In ref 24, an ∼500 fs EET time at 77 K was determined. It appears that more detailed time domain and hole burning studies combined with EET rate calculations are required for an adequate understanding of EET dynamics for excitation at wavelengths shorter than 680 nm.

Acknowledgment. Research at the Ames Laboratory and NREL was supported by the Divisions of Chemical Sciences and Energy Biosciences, Office of Energy Sciences, U.S. Department of Energy, respectively. Ames Laboratory is operated for the U.S. DOE by Iowa State University under contract W-7405-Eng-82. NREL is operated for U.S. DOE by the Midwest Research Institute, Baltelle, and Bechtel under contract D-AC36-99-GO100337. R.P. acknowledges support from MCYT (grant PB98-1632).

References and Notes

(1) Nanba, O.; Satoh, K. *Proc. Natl. Acad. Sci. U.S.A.* **1987**, *84*, 109.
(2) Dekker, J. P.; van Grondelle, R. *Photosynth. Res.* **2000**, *63*, 195.
(3) Prokhorenko, V. I.; Holzwarth, A. R. *J. Phys. Chem. B* **2000**, *104*, 11563.
(4) Zouni, A.; Witt, H. T.; Kern, J.; Fromme, P.; Krauss, N.; Saegner, W.; Orth P. *Nature* **2001**, *409*, 739.
(5) Svensson, B.; Etchebest, C.; Tuffery, P.; van Kan, P.; Smith, J.; Styring, S. *Biochemistry* **1996**, *35*, 14486.
(6) Xiong, J.; Subramanian, S.; Govindjee *Photosynth. Res*. **1998**, *56*, 229.
(7) Deisenhofer, J.; Epp, O.; Miki, K.; Huber, R.; Michel, H.; *J. Mol. Biol.* **1984**, *180*, 385.
(8) Johnson, S. G.; Tang, D.; Jankowiak, R.; Hayes, J. M.; Small, G. J. *J. Phys. Chem.* **1989**, *93*, 5953.
(9) Jankowiak, R.; Hayes, J. M.; Small, G. J. *J. Phys. Chem. B* **2002**, *106*, 8803.
(10) Durrant, J. R.; Klug, D. R.; Kwa, S. L. S.; van Grondelle, R.; Porter, G.; Dekker, J. P. *Proc. Natl. Acad. Sci. U.S.A.* **1995**, *92*, 4798.
(11) Renger, T.; Marcus, R. A. *J. Phys. Chem. B* **2002**, *106*, 1809.
(12) Vacha, F.; Joseph, D. M.; Durrant, J. R.; Telfer, A.; Klug, D. R.; Porter, G.; Barber, J. *Proc. Natl. Acad. Sci. U.S.A.* **1995**, *92*, 2929.
(13) Small, G. J. *J. Chem. Phys.* **1995**, *197*, 239.
(14) Wasielewski, M. R.; Johnson, D. G.; Seibert, M.; Govindjee, *Proc. Natl. Acad. Sci. U.S.A.* **1989**, *86*, 524.
(15) Wiederrecht, G. P.; Seibert, M.; Govindjee; Wasielewski, M. R. *Proc. Natl. Acad. Sci. U.S.A.* **1994**, *91*, 8999.
(16) Schelvis, J. P. M.; van Noort, P. I.; Aartsma, T. J.; van Gorkom, H. J. *Biochim. Biophys. Acta* **1994**, *1184*, 242.
(17) Gatzen, G.; Müller, M. G.; Griebenow, K.; Holzwarth, A. R. *J. Phys. Chem.* **1996**, *100*, 7269.
(18) Greenfield, S. R.; Seibert, M.; Govindjee; Wasielewski, M. R. *J. Phys. Chem. B* **1997**, *101*, 2251.
(19) Groot, M. L.; van Mourik, F.; Eijckelhoff, C.; van Stokkum, I. H. M.; Dekker, J. P.; van Grondelle, R. *Proc. Natl. Acad. Sci. U.S.A.* **1997**, *94*, 4389.
(20) Merry, S. A.; Kamzaki, S.; Tachibana, Y.; Joseph, D. M.; Porter, G.; Yoshohara, K.; Barber, J.; Durrant, J. R.; Klug, D. R. *J. Phys. Chem. B* **1996**, *100*, 10469.
(21) Jankowiak, R.; Tang, D.; Small, G. J.; Seibert, M. *J. Phys. Chem.* **1989**, *93*, 1649.
(22) Tang, D.; Jankowiak, R.; Seibert, M.; Small, G. J. *Photosynth. Res.* **1991**, *27*, 19.
(23) Wasielewski, M. R.; Johnson, D.; Govindjee; Preston, C.; Seibert, M. *Photosynth. Res.* **1989**, *22*, 89.
(24) Visser, H. M.; Groot, M.-L.; van Mourik, F.; van Stokkum, I. H.; Dekker, J. P.; van Grondelle, R. *J. Phys. Chem.* **1995**, *99*, 15304.
(25) Greenfield, S. R.; Seibert, M.; Wasielewski, M. R. *J. Phys. Chem. B* **1999**, *103*, 8364.
(26) Jankowiak, R.; Rätsep, M.; Hayes, J. M.; Zazubovich, V.; Picorel, R.; Seibert, M.; Small, G. J. *J. Phys. Chem. B*, accepted.
(27) Groot, M. L.; Dekker, J. P.; van Grondelle, R.; den Hartog, F. T. H.; Völker, S. *J. Phys. Chem.* **1996**, *100*, 11488.
(28) Völker, S. *J. Lumin.* **1987**, *36*, 251.
(29) van der Zaag, P. J.; Galaup, J. P.; Völker, S. *Chem. Phys. Lett.* **1990**, *174*, 467.
(30) Jankowiak, R.; Rätsep, M.; Picorel, R.; Seibert, M.; Small, G. J. *J. Phys. Chem. B* **1999**, *103*, 9759.
(31) Kwa, S. L. S.; Eijckelhoff, C.; van Grondelle, R.; Dekker, J. P. *J. Phys. Chem.* **1994**, *98*, 7702.
(32) Zazubovich, V.; Jankowiak, R.; Riley, K.; Rätsep, M.; Small, G. J., in preparation.
(33) den Hartog, F. T. H.; Vacha, F.; Lock, A. J.; Barber, J.; Dekker, J. P.; Völker, S. *J. Phys. Chem. B* **1998**, *102*, 9174.
(34) Hayes, J. M.; Lyle, P. A.; Small, G. J. *J. Phys. Chem.* **1994**, *98*, 7337.
(35) Pieper, J.; Voigt, J.; Renger, G.; Small, G. J. *Chem. Phys. Lett.* **1999**, *310*, 296.
(36) Chang, H.-C.; Small, G. J.; Jankowiak, R. *Chem. Phys.* **1995**, *194*, 323.
(37) Tang, D.; Jankowiak, R.; Seibert, M.; Yocum, C. F.; Small, G. J. *J. Phys. Chem.* **1990**, *94*, 6519.
(38) Mukamel, S. *Principles of Nonlinear Optical Spectroscopy*; Oxford University Press: New York, 1995.
(39) Toutounji, M.; Small, G. J.; Mukamel, S. *J. Chem. Phys.* **1999**, *110*, 1017.
(40) Vainer, Yu. G.; Kolchenko, M. A.; Naumov, A. V.; Personov, R. I.; Zilker, S. J.; Haarer, D. *J. Chem. Phys.* **2002**, *116*, 8959.
(41) Reinot, T.; Kim W.-H.; Hayes, J. M.; Small, G. J. *J. Chem. Phys.* **1996**, *104*, 793.
(42) Peterman, E. J. G.; van Amerongen, H.; van Grondelle, R.; Dekker, J. P. *Proc. Natl. Acad. Sci. U.S.A.* **1998**, *95*, 6128.
(43) Durrant, J. R.; Hastings, G.; Joseph, D. M.; Barber, J.; Porter, G.; Klug, D. R. *Proc. Natl. Acad. Sci. U.S.A.* **1992**, *89*, 11632.
(44) Greenfield, S. R.; Seibert, M.; Govindjee; Wasielewski, M. R. *Chem. Phys.* **1996**, *210*, 279.
(45) Roelofs, T. A.; Kwa, S. L. S.; van Grondelle, R.; Dekker, J. P.; Holzwarth, A. R. *Biochim. Biophys. Acta* **1993**, *1143*, 147.
(46) Holzwarth, A. R.; Müller, M. G.; Gatzen, G.; Hucke, M.; Griebenow, K. *J. Lumin.* **1994**, *60*, 497.